# SOME EXPLORATION APPLICATIONS OF THE TWO-DIMENSIONAL FOURIER-TRANSFORM*

by

J. C. DEN BOER

*ABSTRACT*

The basic mathematical relationships of the one-dimensional Fourier-Series and Transform are reviewed in a heuristic manner.

The two-dimensional Fourier Transform is shown to be a natural extension of its one-dimensional equivalent by means of an example from seismic exploration.

Several applications of the two-dimensional transform, in the field of exploration geophysics, are discussed and illustrated.

The subject of the Fourier Transform, notwithstanding its fundamental importance in many aspects of geophysical data-analysis, has been much neglected and avoided for a long time by Operations departments engaged in exploration geophysics. However, with the large-scale introduction of digital computers in geophysical exploration during the past few years, the Fourier Transform has gained a considerable amount of attention. In particular, the fairly recent concept of the Fast Fourier Algorithm (FFT), which permits rapid calculation of the transforms even on small-size computers, has contributed much to this renewed interest in transform mathematics.

In order to establish at least some form of foundation for the two-dimensional transform it may be advisable to briefly review the fundamentals of the one-dimensional Fourier series and transforms. Of necessity we will have to sacrifice mathematical rigourousness for speed. In other words we will use the heuristic explanation which is nothing more than the scientific term for a "seat of the pants" approach. In essence the philosophy of the Fourier series implies that a non-analytical function can nevertheless be closely approximated by an analytical expression. In particular, the Fourier series states that such a function may be approximated by the summation of a large number of sine-and cosine waves of different frequencies, amplitudes and phases.

In the following discussions we will initially utilize functions for which the independent variable is "time." The main reason for this choice is the fact that we will also be concerned with an associated variable which has the inverse dimension. The inverse of time, of course, has the dimension of frequency. However, there is nothing magical about the choice of independent variable: one could choose distance and the inverse would be spatial frequency or wave-number.

Figure 1 shows the basic mathematics of the Fourier series for both real and complex, periodic functions. Note that the real function is a

*Lecture presented at the University of British Columbia, March 1967, by Dr. J. C. den Boer, Mobil Oil Canada Ltd.

COMPLEX

$$f(t) = \sum_{n=-\infty}^{+\infty} (A_n \cos \omega_n t + B_n \sin \omega_n t)$$

REAL

$$f(t) = \frac{A_0}{2} + \sum_{n=1}^{\infty} (A_n \cos \omega_n t + B_n \sin \omega_n t)$$

by vector addition of sine and cosine :

$$f(t) = \sum_{n=-\infty}^{+\infty} F_n \cos (\omega_n t - \Theta_n)$$

$$f(t) = \frac{A_0}{2} + \sum_{n=1}^{\infty} F_n \cos (\omega_n t - \Theta_n)$$

$$F_n = \sqrt{A_n^2 + B_n^2}$$

$$\Theta_n = \tan^{-1} \frac{B_n}{A_n}$$

$$A_0 = \frac{1}{T} \int_{-T/2}^{+T/2} f(t)\, dt$$

$$A_n = \frac{1}{T} \int_{-T/2}^{+T/2} f(t) \cos \omega_n t\, dt$$

$$A_n = \frac{2}{T} \int_{-T/2}^{+T/2} f(t) \cos \omega_n t\, dt$$

$$B_n = \frac{1}{T} \int_{-T/2}^{+T/2} f(t) \sin \omega_n t\, dt$$

$$B_n = \frac{2}{T} \int_{-T/2}^{+T/2} f(t) \sin \omega_n t\, dt$$

FIG. 1.—Fourier Series periodic functions.

special case of the complex one. For this reason we will limit ourselves to the discussion of complex functions only since they constitute the general case. The series may be written as a summation of sine and cosine waves, or alternately via vector-addition, as a sum of cosine waves only. The coefficients of the series, $A_n$ and $B_n$, can be calculated by evaluating the integral equations shown over the duration of one full period. For non-analytical functions f(t) this evaluation will generally be achieved by means of numerical methods.

An illustration of a periodic time-function and its individual Fourier components is shown in Figure 2. Each component is a sine or cosine wave of discrete frequency, amplitude and phase. In this example only 10 component-waves were used, nine of which have the same amplitude but different phase. It will be clear that in this manner any arbitrary, but periodic, waveform may be approximated by a large number of component waves. The mathematical relationships, shown in Figure 1, are only applicable to periodic functions and are not valid for fairly arbitrary non-periodic (transient) functions.

Figure 3 indicates how the Fourier techniques apply to the class of non-periodic functions. By letting the period T approach infinity, the coefficients $A_n$ and $B_n$, which previously referred to discrete frequencies, now become continuous functions of frequency ($\propto$(f) and $\beta$(f) respectively) and the integrations must be carried out from minus-infinity to

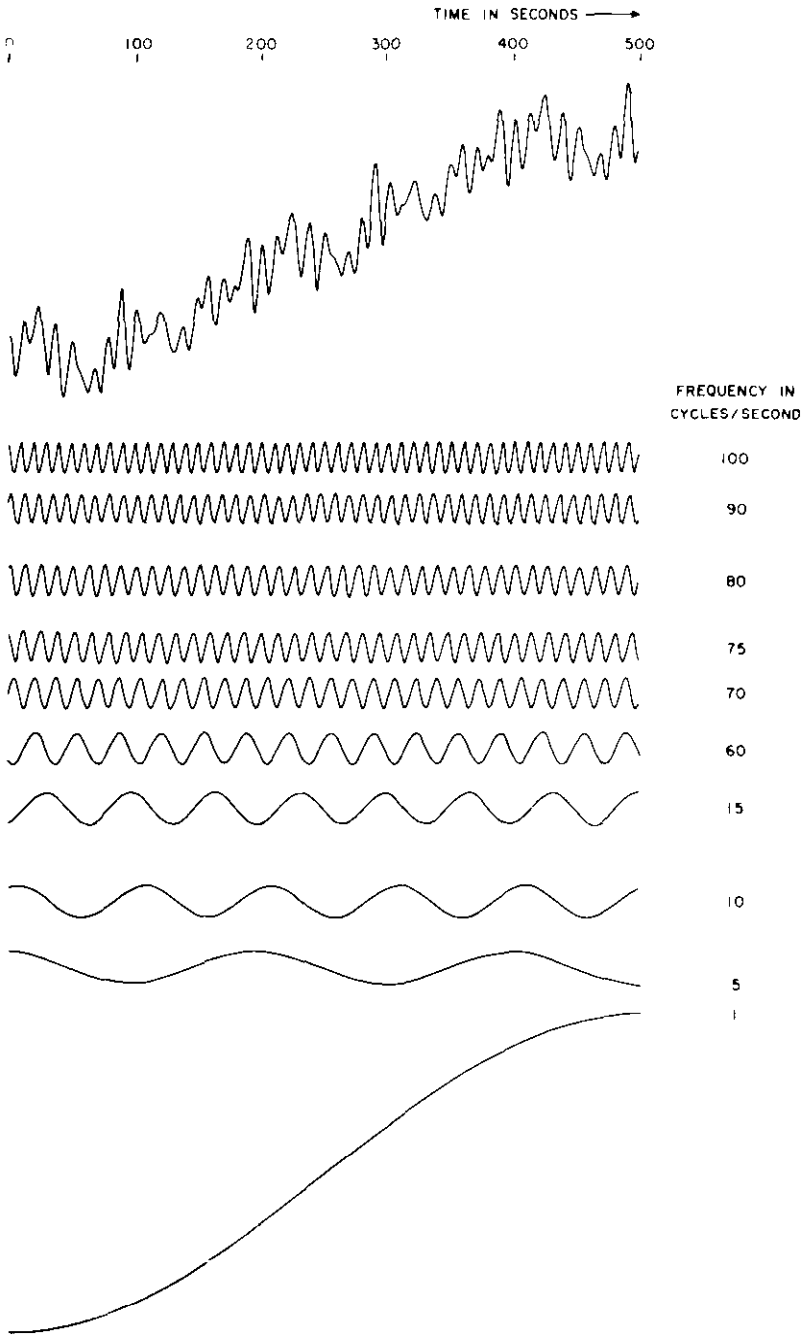


FIG. 2.—Fourier Analysis/Synthesis.

PERIOD $T \to \infty$, therefore $A_n \to \alpha(f)$ and $B_n \to \beta(f)$, continuous functions of frequency.

$$\alpha(f) = \int_{-\infty}^{+\infty} f(t) \cos \omega t \, dt \qquad \beta(f) = \int_{-\infty}^{+\infty} f(t) \sin \omega t \, dt$$

via Euler's rule : $e^{-j\omega t} = \cos \omega t - j \sin \omega t$

FOURIER TRANSFORM : $F(f) = \int_{-\infty}^{+\infty} f(t) e^{-j\omega t} dt$, INVERSE TRANSFORM : $f(t) = \int_{-\infty}^{+\infty} F(f) e^{j\omega t} df$

where

Complex Spectrum..... $F(f) = |F(f)| e^{j\Theta(f)}$

Amplitude Spectrum..... $|F(f)| = \sqrt{\alpha^2_{(f)} + \beta(f)^2}$

Phase Spectrum..... $\Theta(f) = \tan^{-1} \dfrac{\beta(f)}{\alpha(f)}$

FUNDAMENTAL THEOREM :

Filtering (Convolution) :

$O(t)_{\text{Output}} = I(t)_{\text{Input}} * G(t)_{\text{Filter Response}}$ ..... Time domain

$O(f) = I(f) \cdot G(f)$ ..... Frequency domain

FIG. 3.—Fourier integral transient functions.

plus-infinity. Again, through vector addition of sine and cosine waves (Euler's Rule), the $\alpha$ and $\beta$ coefficients may be combined into one equation which then assumes the form of the well-known Fourier Integral or to put it in the proper terminology for our purpose, the one-dimensional Fourier Transform. The derivation of the Fourier transform from the Fourier series, while not difficult in any way, is not always well understood. For this reason the mathematical relationships effecting this derivation are included in the Appendix.

Just as the Fourier Transform describes the analysis of a time function in its individual frequency components (Fourier analysis), the Inverse Fourier Transform synthesizes the time function from the constituent frequency components. From the appearance of the two transforms it is easily seen that two successive transformations will yield the original time-function within a constant factor. The quantity F(f) is called the Fourier Transform of f(t) or the Complex Spectrum of f(t) since it consists of both a real and imaginary part. Considering the vectorial presentation of a complex number in the complex plane we can assign an absolute value (length of the vector) to the Complex Spectrum, $|F(f)|$, which is generally referred to as the Amplitude Spectrum or Amplitude Response. The angle between the vector and the real-axis constitutes the Phase Spectrum or Phase Response.

Having established the Fourier Transform and its components at this stage, let us recall briefly (Figure 3) an important fundamental theorem of the transform, which is quite pertinent to Geophysical applications (filter theory): the mathematical process, whereby an input time-function is filtered by another time-function to produce an output time-function, is known as *convolution.* This operation is performed in, what is properly called, the *Time-domain.* Utilizing the Fourier transform, this process can also be described in the *Frequency-domain,* as follows: the transform of the output equals the product of the transforms of input and filter. Or, in other words, convolution in the time-domain is multiplication in the frequency-domain.

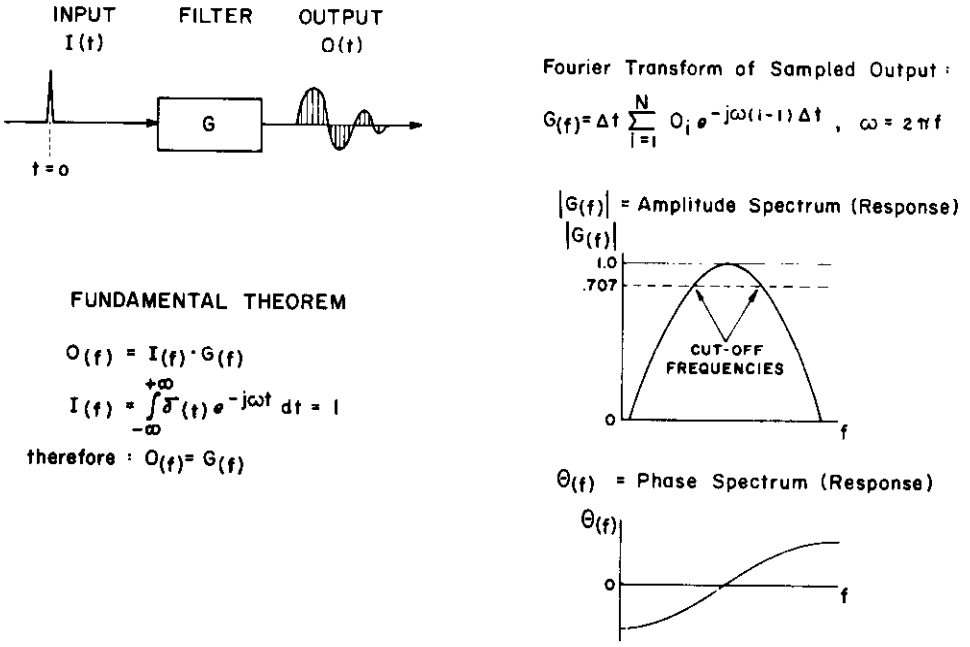


FIG. 4.—Electrical filter (frequency filter).

Figure 4 illustrates an immediate application of the Fourier Transform and the fundamental theorem stated previously. If the input to an electrical filter G consists of a spike or delta-function, then the transform of the output is equal to the product of the transforms of the filter response and the delta-function. As shown in Figure 4, the transform of the latter equals one and therefore the transform of the output is equal to the Transfer function of the filter (transform of filter impulse response). Alternately, the output in the time-domain represents the filter's Impulse response. The filter Transfer function (Complex Spectrum) may be evaluated by sampling the Impulse response and evaluating the Fourier transform on the sampled function. Figure 4

shows that the Fourier Integral assumes the form of a summation over the time duration of the waveform. Again the Complex Spectrum (Transfer Function) may be characterized by its absolute value or Amplitude Response and Phase Response. The Amplitude Response is generally used to identify the characteristics of an electrical filter which is usually specified by its Cut-off frequencies (the frequencies at which the amplitude has a value of .707) or Half-power points. In order to demonstrate that there is nothing magical about the choice of independent variable, let us now consider a case where this variable is "distance."

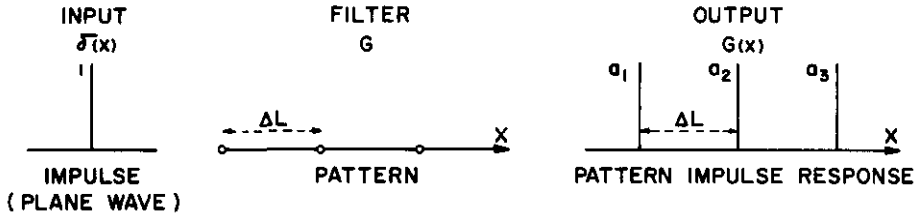


$$G(x) = a_1\delta(x) + a_2\delta(x-\Delta L) + a_3\delta(x-2\Delta L)$$

$$G(k) = \int_{-\infty}^{+\infty}\left[a_1\delta(x) + a_2\delta(x-\Delta L) + a_3\delta(x-2\Delta L)\right]e^{-j\omega x}\,dx$$

where: $k$ = apparent wavenumber (spatial frequency)

$\omega = 2\pi k$

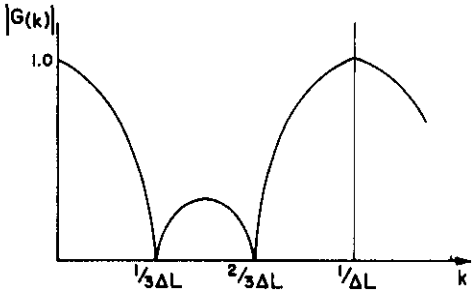


FIG. 5.—Geophone pattern (wave-number filter).

Figure 5 illustrates the situation where an impulsive, horizontally travelling plane wave passes a linear array of three geophones at regular spacing $\Delta l$. Assuming that the geophones are not identical the impulse response of the pattern will consist of three spikes of amplitudes $a_1$, $a_2$, and $a_3$ at regular spacing $\Delta l$. The impulse response, therefore, is a function in the "distance-domain." Evaluation of the Fourier Transform of the Pattern impulse response will provide us with the Pattern response in the inverse domain, the "wave-number (spatial frequency) domain." The integration in Figure 5 can be easily carried out, since it is analytical, and will yield the Complex Spectrum of the geophone pattern. Calculation of the absolute value, the Amplitude Response of the Pattern, yields the well-known Response curve shown

in Figure 5. The Amplitude response characterizes the geophone pattern as a wave-number filter that will pass certain wave-numbers and attenuate others.

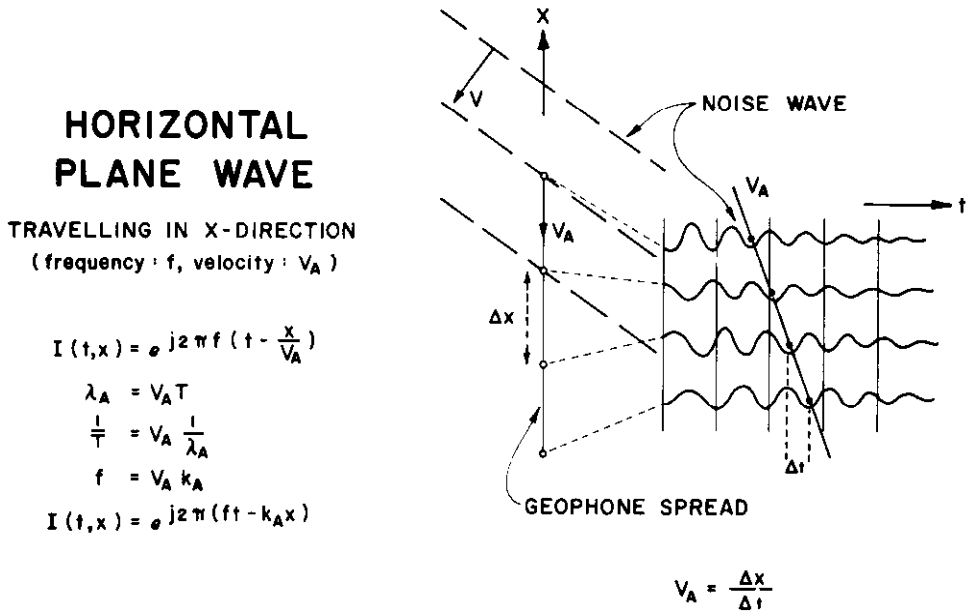


Fig. 6.—Horizontal plane wave travelling in X-direction.

Let us pursue the subject of the horizontally travelling plane wave somewhat further since it will serve admirably as an introduction of the two-dimensional Fourier Transform, our main topic. Figure 6 shows such a wave, for example a surface noise-wave in seismic exploration, passing a spread of geophones at a certain velocity V. The mathematical expression for such an event is indicated on Figure 6 but is immaterial for the following discussion.

To the extreme right on this figure is shown a typical seismic record which could be generated by the arrival of the noise-wave at the geophone spread. Judging from the arrival-times at successive geophones the noise-wave is travelling across the spread with an apparent velocity $V_A$ which may be determined from the known geophone spacing $\Delta x$ and the time stepout from trace to trace ($\Delta t$). Through the period T of the noise-wave, observed on the record, and the apparent velocity $V_A$ we can associate an apparent wave-number $K_A$ with the noise-train. *We are thus faced with a situation where the characteristics of the noise-wave are established, not from one single trace, but from a multitude of traces resulting from a geophone spread on the ground.*

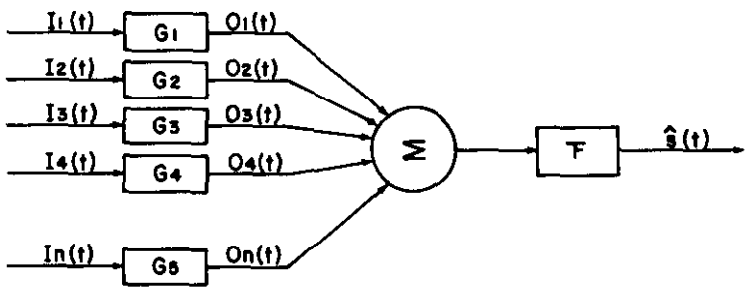


HORIZONTAL PLANE WAVE : $I_n(t) = e^{j2\pi(ft-kx)}$

x constant (single trace) : $I_n(f) = \int_{-\infty}^{+\infty} e^{j2\pi(ft-kx)} e^{-j2\pi ft}\, dt$

t constant (multi trace) : $I_n(k) = \int_{-\infty}^{+\infty} e^{j2\pi(ft-kx)} e^{-j2\pi kx}\, dx$

TWO DIMENSIONAL FOURIER TRANSFORM : $I(f,k) = \iint I(t,x)\, e^{-j2\pi(ft+kx)}\, dt\, dx$

Two Dimensional Complex Spectrum is function of both frequency and wave-number

INVERSE TRANSFORM : $I(t,x) = \iint I(f,k)\, e^{j2\pi(ft+kx)}\, df\, dk$

FIG. 7.—Multi-channel filter.

Here then we are confronted with the subject of multi-channel or multi-trace operations. Figure 7 illustrates the general philosophy of multi-channel filtering operations: a selected number of traces is filtered individually by a set of filters (one for each channel) which are designed to achieve a specified objective in an optimum manner. The outputs of all filters are summed and then filtered by an optimum inverse filter to yield the best estimate of the signal (on a single trace) under conditions of optimum attenuation of noise. For example, returning to the horizontally travelling noise-wave, the objective of the multi-channel processor could be the attenuation of the coherent noise event from the array of traces and to yield a single output trace containing the signal uncorrupted by the noise-train.

Using the one-dimensional Fourier Transform for a single trace (independent of distance x) yields the Complex Spectrum as a function of frequency f, just as some of our previous examples. However, by considering the array of traces only (keeping time t constant) the Fourier Transform becomes a function of wave-number only. Obviously, one must consider both variables, distance and time simultaneously which can easily be achieved by combining the two one-dimensional transforms into one two-dimensional Fourier Transform. *The two-dimensional*

*Complex Spectrum, therefore, is a function of both frequency and wave-number.* Analogous to the one-dimensional case, the transform-pair is completed by the two-dimensional inverse transformation.

As in the cases of the electrical (frequency) filter and geophone pattern (wave-number) filter, where we studied their Amplitude response in terms of frequency versus amplitude and wave-number versus amplitude, we would like to investigate the Amplitude Response of the multichannel processor in terms of both frequency and wavenumber versus

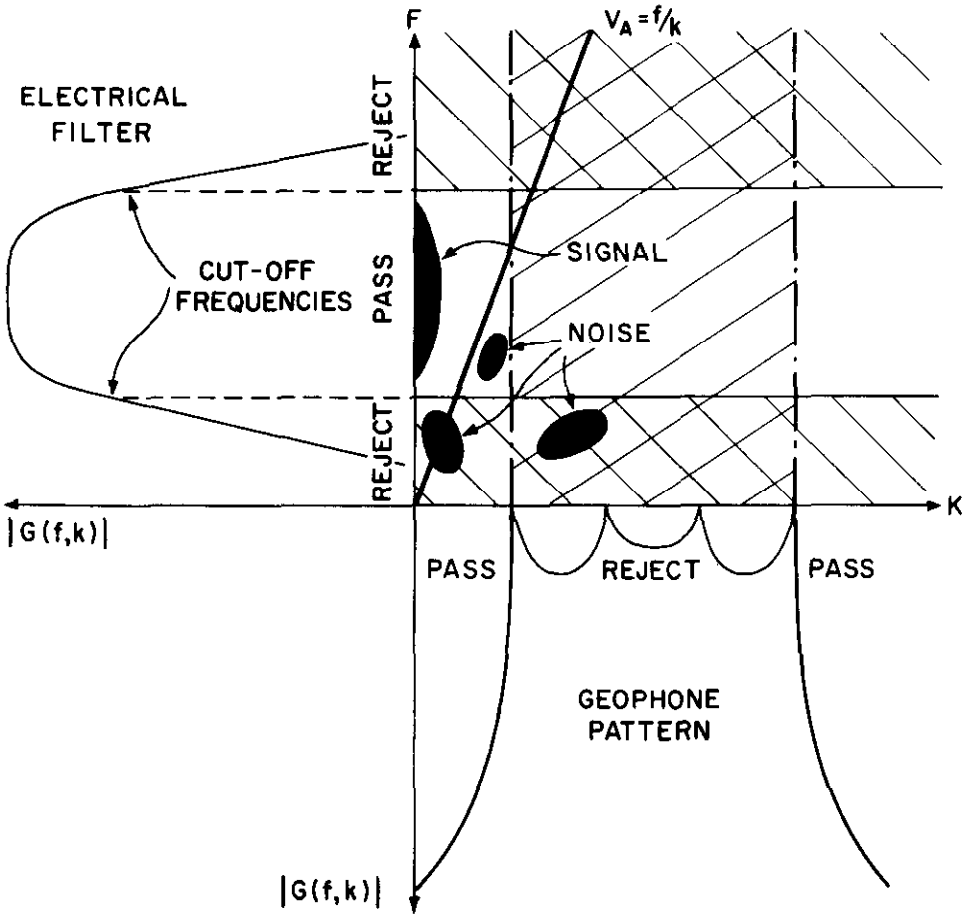


FIG. 8.—Components of F-K plot.

amplitude. Figure 8 illustrates how such an analysis is conveniently achieved by an F-K plot on which the amplitude response is contoured since the amplitude constitutes the third dimension of the plot, perpendicular to Figure 8. (Generally in the form of decibels attenuation.) For purposes of investigation we have indicated areas of F-K space in which (seismic) signal and noise could be located. Seismic reflection energy, by its nature of near-vertical incidence, will show very little or no step-out from trace to trace. This of course assumes that the reflecting beds have little or no dip. Therefore, the apparent velocity with which the reflection will move across a geophone spread is infinite or at least very large. The associated wave-number, therefore, will be zero or near-zero as shown on Figure 8 (SIGNAL). Reflection energy, generally, contains predominant frequencies in the range between 20-60 cycles per second. Horizontally travelling noise-waves, however, will have a distinct range of non-zero wave-numbers depending on the apparent velocity with which they travel across the spread. On the other hand, surface waves contain predominant frequencies in the range below 20 cycles per second.

For these reasons reflection energy and surface waves may occupy distinctly different positions in F-K space (Figure 8). In order to better understand the components of an F-K plot let us first consider the frequency versus amplitude aspects. (For purposes of display the A-F and A-K coordinate plane have been "folded" in the F-K plane.) Previously we have seen that the Amplitude Response of the electrical (frequency filter) fits this category eminently. Figure 8 shows that the cut-off frequencies of the electrical filter constitute straight lines (2) parallel to the wave-number axis on the F-K plot, dividing the F-K space in a "pass" and two "reject" areas.

Similarly, by considering the amplitude versus wave-number coordinate plane only, we are confronted once more with the Amplitude Response of the geophone pattern (wave-number filter). In this case the cut-off frequencies on the F-K plot are represented by two straight lines parallel to the frequency axis dividing the F-K space in two "pass" areas and one "reject" area.

Knowing the position of signal and noise on the F-K plot, (Figure 8) through the analysis of a noise spread, an optimum combination of electrical recording filter and geophone pattern may be established through judicious choice of cut-off frequencies for both filters. However, there is a practical limit to this choice dictated by operational feasibility. In general it is very undesirable to record with a narrow-band electrical filter while a large number of geophones in the pattern hampers field operations. A typical example of this dilemma is illustrated on Figure 8 by the uppermost of the three noise-patches. For the chosen electrical filter and geophone pattern this noise falls in the pass-band of both filters. Assuming that further narrowing of either pass-band is undesirable, the only way of attenuating this noise would be through a filter with a cut-off following radial lines on the F-K plot, as indicated. Such a radial line through the origin is representative

of apparent velocity $V_A$ since it represents the equation $F/K = \text{constant}$. The desired filter would therefore discriminate on the basis of apparent velocity and is most properly called a "Velocity filter." (Also called "fan-filters.")

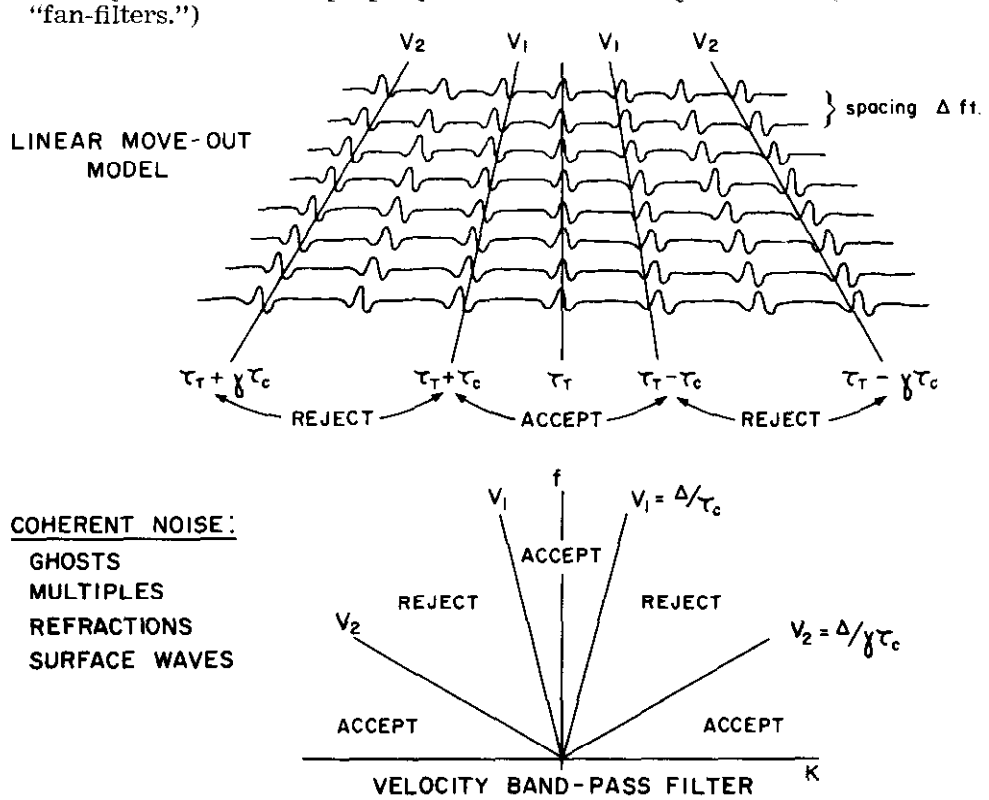


FIG. 9.—Velocity filter to attenuate coherent noise events.

We have essentially described the Velocity filter operation in our discussion of the multi-channel filter for a horizontally travelling noise-wave. Suffice it to say that, through the mathematics of Optimum inverse filter generation according to Wiener's theory, it is possible to establish a number of filters (one for each channel) which will attenuate certain apparent velocities (step-outs) across a seismic record and pass others with a minimum of distortion (Figure 9). Noise events falling in the category of coherent noise with step-outs different from reflection step-outs are well-known in the form of multiple reflections, ghosts, refractions and surface waves. The simplest Velocity filter, the band-pass filter is illustrated in Figure 9. On the linear move-out model (a seismic record after Normal Moveout correction) it will reject any events exceeding a specified step-out of $\tau_c$ milliseconds per trace-interval and will pass any event with less move-out. The characteristics of the filter are schematically indicated in the F-K plot at the bottom of Figure 9.

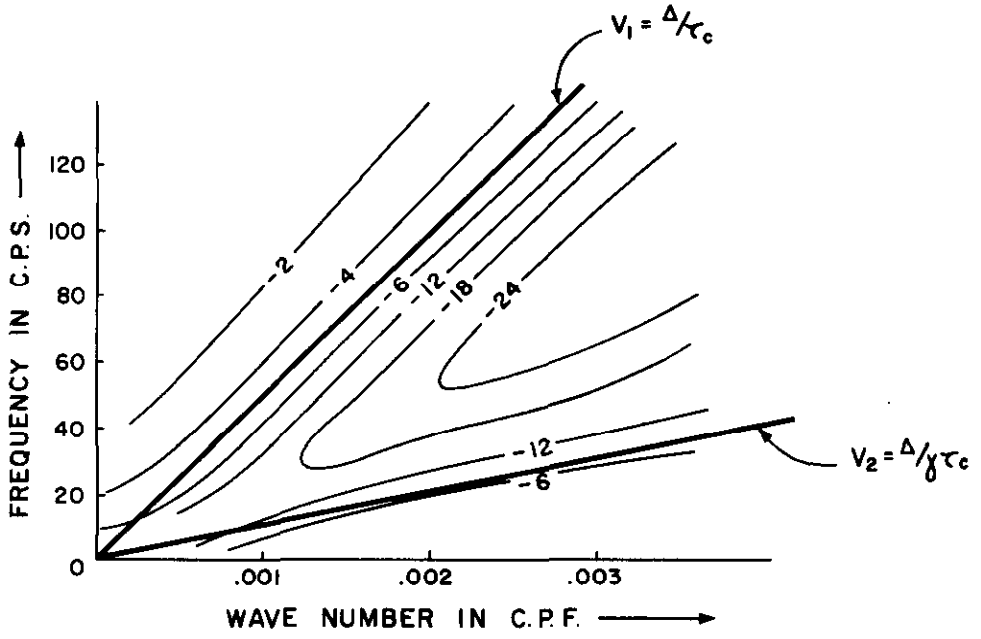


FIG. 10.—Typical F-K plot velocity filter response (contoured in db).

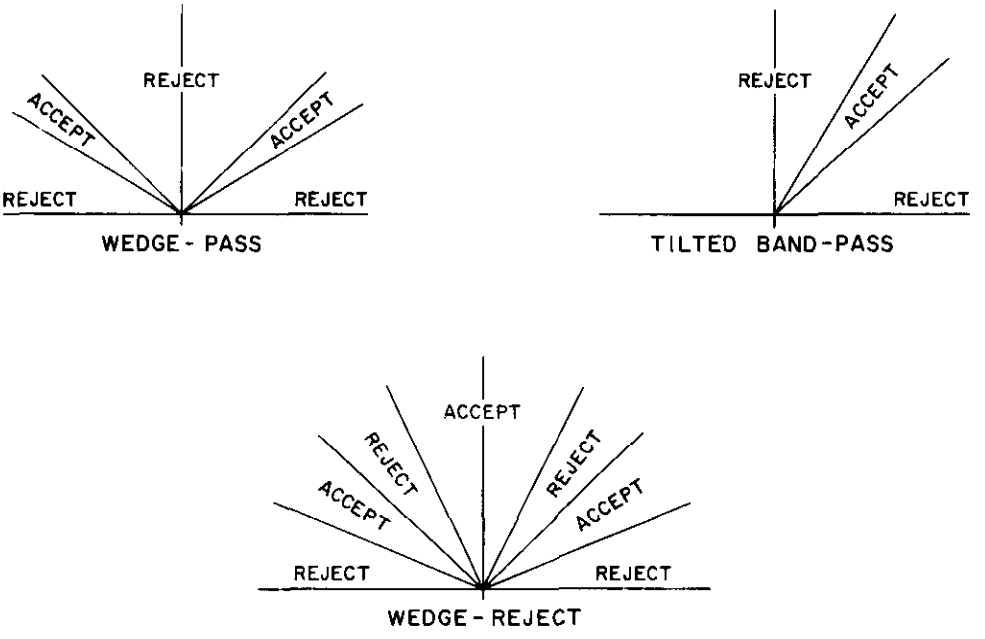


FIG. 11.—Different types of velocity filter.

A typical Velocity Band-pass filter Amplitude Response is shown in Figure 10. The response is quite flat in the pass-band showing only minor attenuation. Attenuation increases rapidly across the cut-off velocity and reaches a maximum of 24 db in the reject-band.

Figure 11 illustrates, diagrammatically, the amplitude response of several types of velocity filters which are currently being used for Geophysical Data Processing: the wedge-pass filter, the tilted band-pass and the wedge-reject filter.

A discussion of multi-channel Velocity filters today cannot be complete without mention of a recent development in the field of Industrial Optics: the Laser Scan.

The following set of figures, describing the principles of the Laser-Scan, are based on the excellent discussion of the equipment by Dobrin et al., 1965.

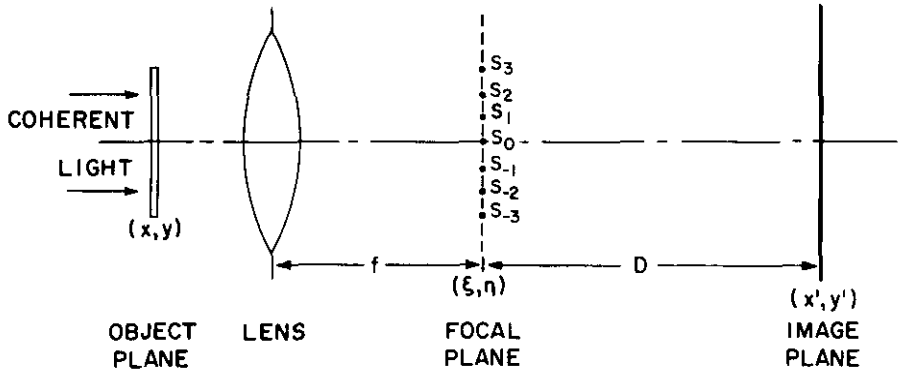


DIFFRACTION PATTERN ($S_0, S_1, S_{-1}$, etc.): $U(\xi,\eta) = C_1 \iint F(x,y)\, e^{jk(\xi/f \cdot x + \eta/f \cdot y)}\, dx\, dy$

$f$ = focal length
$k$ = wave number
$C_1$ = constant

IMAGE PLANE: $V(x',y') = C_2 \iint U(\xi,\eta)\, e^{-jk(x'/D \cdot \xi + y'/D \cdot \eta)}\, d\xi\, d\eta$

$C_2$ = constant
$D$ = distance focal plane - image plane

IMAGE - OBJECT: $V(x',y') = C\,F(x,y)$, $C = C_1 C_2 \lambda^2 f^2$

$\lambda$ = wave length

FIG. 12.—Abbe's Theory (1873) (after Dobrin et al.).

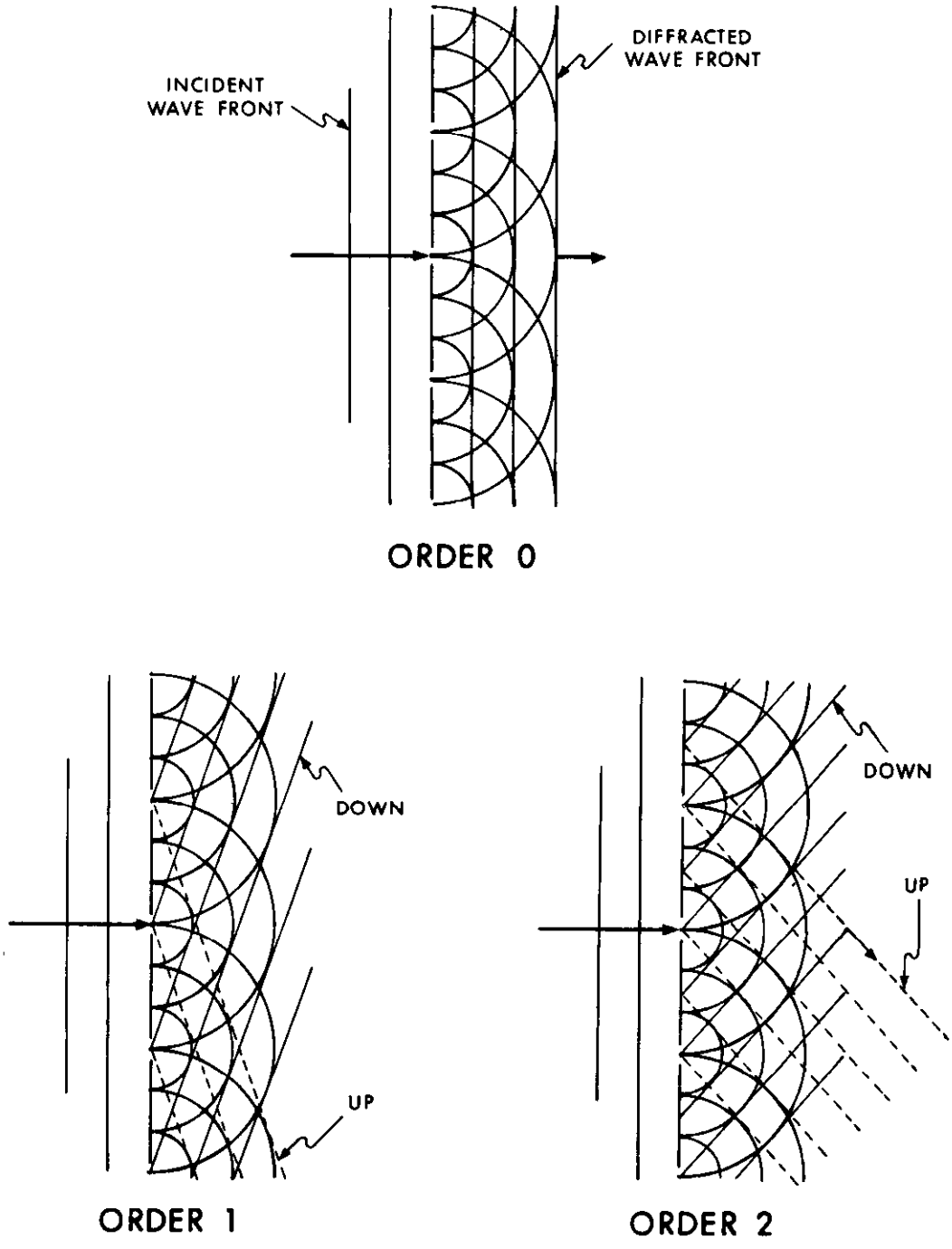


FIG. 13.—Wave front diffraction through slitted grating (after Dobrin et al.)

Figure 12 shows, diagrammatically, the fundamental background of this optical equipment. Coherent light passing through a diffracting medium and a spherical or cylindrical lens will give rise to a diffraction pattern in the focal plane of that lens. According to Abbe (1873) the diffraction pattern is expressible in the form indicated on Figure 12. One needs little imagination to realize that this expression is nothing but a two-dimensional Fourier Transform. In other words, the diffraction pattern in the focal plane of the lens is the two-dimensional Fourier Transform (Complex Spectrum) of the light distribution in the diffraction grating. The image of the object (a reproduction of the "slitted" grating) is formed in a similar manner by an inverse transformation of the diffraction pattern in the focal plane of a second lens. While a rigorous derivation of these relationships is entirely outside the scope of this discussion, the transformation principle may be arrived at intuitively through the following qualitative reasoning. It is well known, that the spacing of the diffractions from a "slitted" grating is inversely proportional to the spacing of the slits. Therefore, if the "slits" are spaced in units of distance, the diffractions will be spaced in units of wave-number (inverse of distance). Alternately, if the "slits" are spaced in units of time, then their diffractions will be spaced in terms of frequency. This, of course, is entirely analogous to the transformation inherent to the Fourier transform.

Figure 13 illustrates in some detail how a diffraction pattern is generated by a plane wave of coherent light passing through a grating. Each slit will act as a secondary source of wave generation according to Huygen's principle. The wave-fronts from adjacent slits will interfere in a constructive sense, each combination being responsible for a different order diffraction. The diffractions of zero, first, and second order are indicated on Figure 13.

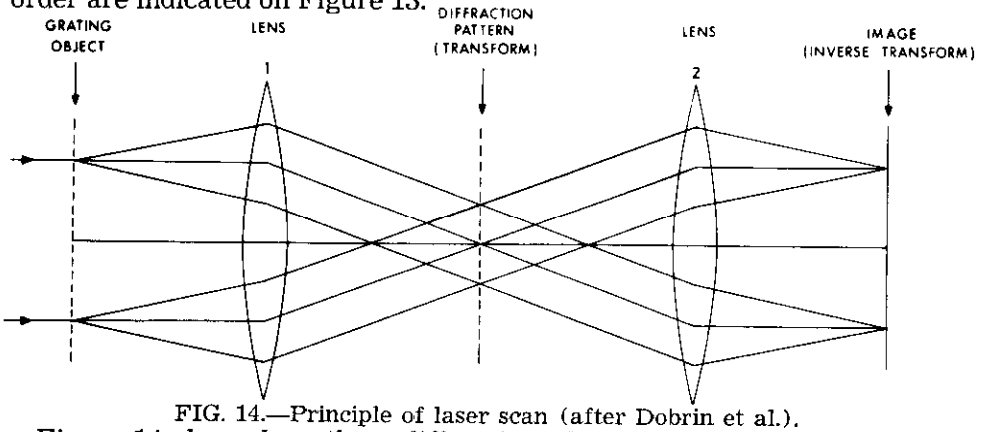


FIG. 14.—Principle of laser scan (after Dobrin et al.).

Figure 14 shows how these diffractions, by passing through a spherical lens, will each converge to a dot in the focal plane of the lens thus giving rise to the Fourier transform of the data. Note that the plane containing the dots is perpendicular to the direction of the diffracting slits. A second lens system, identical to the first, will perform the inverse transformation and produce the image of the diffraction grating

in the focal plane of the second lens. If no light in the diffraction pattern is obstructed, the image will be identical to the object. However, if any portion of the pattern is blocked off (light filtered out) in the transform plane, the image will be identical to the object with the exception of the parts associated with the blocked diffractions.

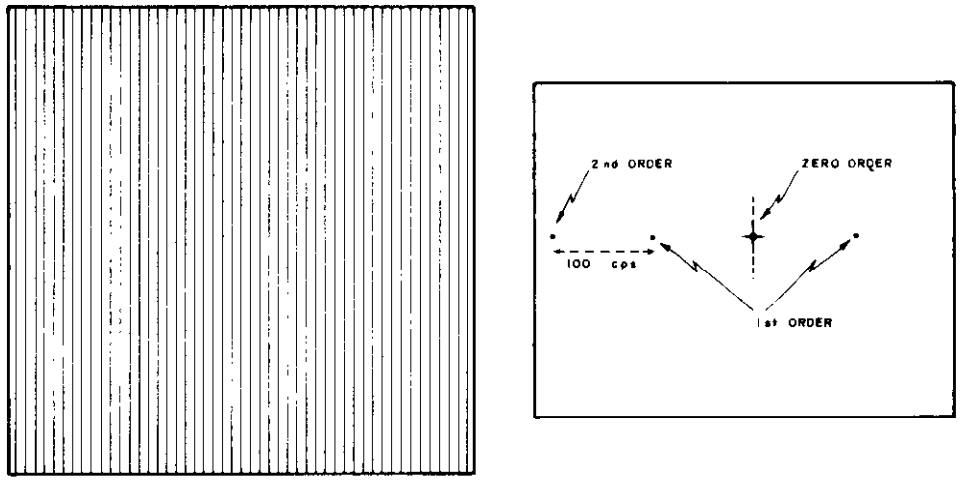


DIFFRACTION GRATING
Timing lines at .010 sec. spacing

DIFFRACTION PATTERN
(FOURIER TRANSFORM)

FIG. 15.—(After Dobrin et al.).

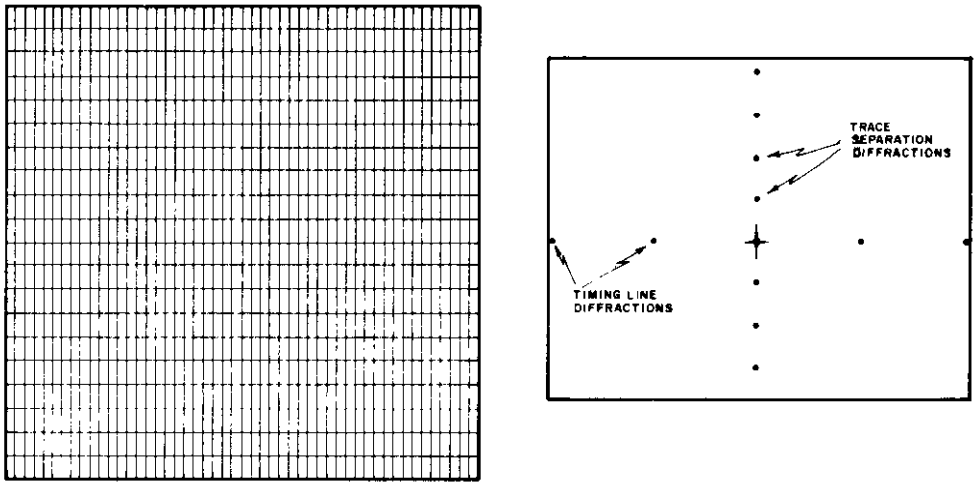


DIFFRACTION GRATING
Timing lines at .010 sec spacing
and trace separations at Δx feet.

DIFFRACTION PATTERN
(FOURIER TRANSFORM)

FIG. 16.—(After Dobrin et al.).

Figure 15 is an example of the two-dimensional transform, generated by the Laser Scan, from a diffraction grating consisting of a 35 MM photo-transparency of a set of closely spaced lines. The diffraction grating, in this case, represents a hypothetical seismic record section consisting of timing lines only. Since the timing-lines are spaced in time (f.e. .010 sec.) the diffraction dots are spaced in frequency (i.e. 100 cycles/sec.) in the transform-plane.

On Figure 16 a perpendicular pattern of lines has been added representing channel (trace) separations. Since the traces or channels are spaced in feet, their diffraction patterns in the transform-plane are spaced in terms of wave-number. Here then we are confronted with the fact that a seismic record section, consisting of timing-lines and traces will generate a diffraction pattern in the transform-plane which is nothing else but our previously discussed F-K plot for which, in this case, the F and K axes are even calibrated in terms of frequency and wave-number respectively.

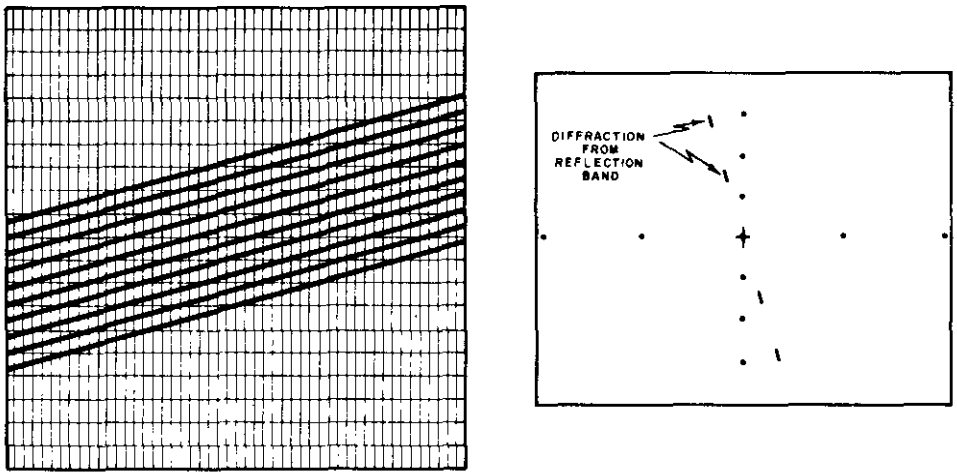


FIG. 17.—(After Dobrin et al.).

On Figure 17 yet another pattern is added to simulate a set of dipping reflections in the form of a variable area presentation. It is easily seen that such a set of events could be caused for example by horizontally travelling noisewaves as discussed previously. A third diffraction pattern, along a radial direction, is clearly indicated. Therefore, if the diffraction grating consists of a 35 MM photo-transparency of a variable area seismic record section, the diffraction pattern in the focal plane

of the lens will be the two-dimensional Fourier transform of that record section in the form of an F-K plot. The filtering operations discussed before (frequency, wave-number, velocity-filter) can be easily performed with the Laser Scan by physically blocking the diffractions of undesired events in the transform plane. Recalling our previous discussion of filter cut-off frequencies in F-K space, it is easily seen that the equiv-

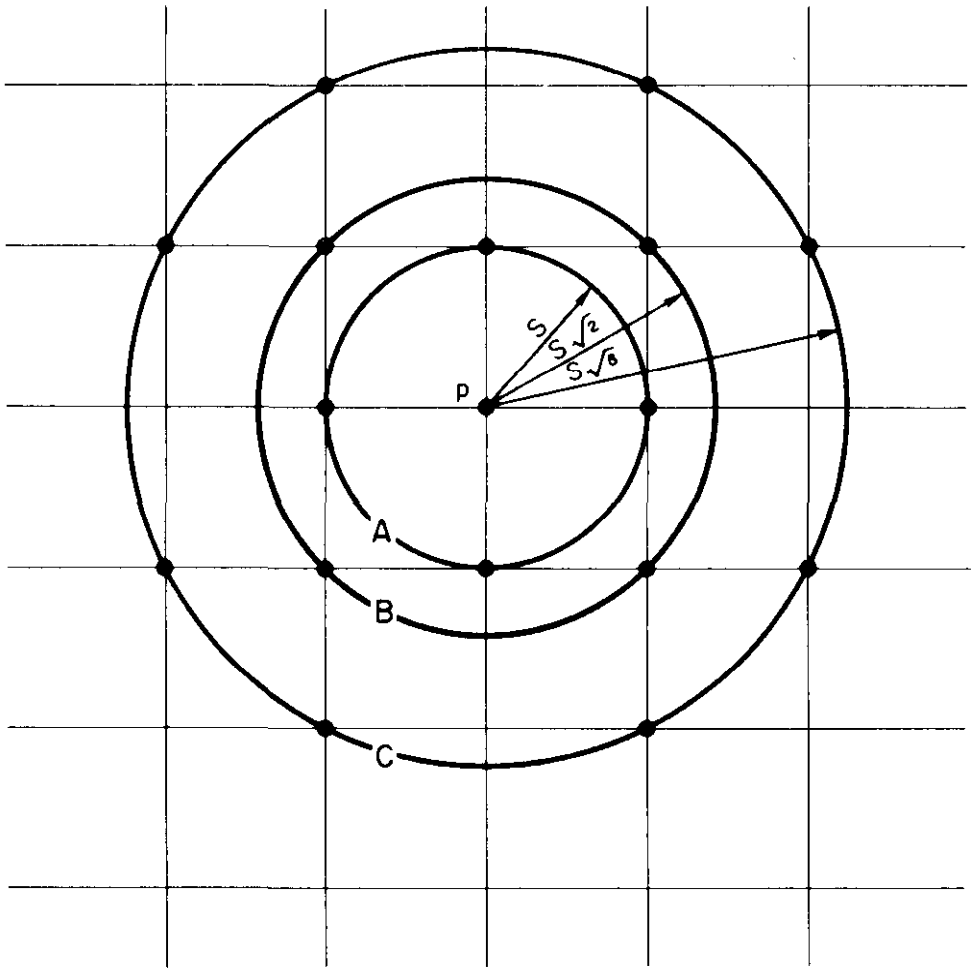


$$\left\{\frac{\partial^2 g}{\partial z^2}\right\} p \approx \frac{1}{24 S^2}\left[96 g_p - 18\sum_A g(S) - 8\sum_B g(S\sqrt{2}) + \sum_C g(S\sqrt{5})\right]$$

FIG. 18.—Computation diagram for the second vertical derivative of gravity after Rosenbach - Elkins.

alent filtering on the Laser Scan can be achieved simply by two sets of knife edges, one horizontal for the frequency filter, one vertical for the wave-number filter and a set of physical wedges of different apertures for the velocity-filters. There cannot be much doubt, therefore, that the Laser Scan is an excellent example of an Exploration application of the two-dimensional Fourier Transform.

So far, we have only discussed applications of the Transforms in the field of Seismic Data Processing. For our last example, let us consider an interesting use of the Transform relating to the analysis of Potential field data (both gravity and magnetics). The usefulness of Derivative and Continuation techniques, as tools for providing greater resolution in Potential Field data, has been recognized for quite some time. The literature on this subject is as voluminous as the number of different numerical techniques that have been proposed *and used.* Many rather heated discussions have taken place in the past with respect to the relative merits of the individual approaches, but most arguments were somewhat futile due to a lack of quantitative comparisons of the techniques. It is only fairly recent that the industry has realized that such numerical schemes are essentially two-dimensional spatial filters and therefore subject to Amplitude Response analysis through Fourier Transforms (Fuller, 1966, Zurflueh, 1967, Darby & Davies, 1967).

Figure 18 is a typical example of a numerical filter designed to calculate the Second Vertical Derivative of gravity data. The majority of current techniques assumes that the potential field has been observed or interpolated on a regular square grid of certain unit spacing. The observed values at selected gridpoints are multiplied by predetermined coefficients (are weighted) and the resulting products are summed to produce the second vertical derivative at the centre of the configuration (template). It is important to remember that all such techniques utilize templates with a radial symmetry. The weighting coefficients of symmetrically located points in each of the quadrants are identical.

Since the Second Vertical Derivative is a two-dimensional spatial filter we may investigate its spatial frequency (or wave-number) response through the two-dimensional Fourier Transform (Fig. 19). In Figure 19 the spatial filter is characterized by $f(x, y)$ and its Complex Spectrum by $F(k_x, k_y)$. The radial symmetry of the filter may be expressed mathematically by stating that $f(x, y)$ is an even function in both x and y. This in turn means that the Spectrum is real and contains no imaginary part. The two-dimensional Fourier Transform can therefore be simplified as indicated on Figure 19. Essentially, the filter function $f(x, y)$ consist of a number of weighting coefficients to be assigned to the data values at discrete gridpoints with coordinates $(n\Delta x, m\Delta y)$ with respect to the gridpoint where the output is desired. We may therefore replace the integrations over the dimensions of the template by summations over the number of gridpoints involved. The weighting coefficient at any gridpoint $(n, m)$ may be designed as $W(n, m)$ and the Fourier Transform can be easily evaluated as the double summation of Figure 19.

$$\text{FILTER TRANSFORM} : F(k_x,k_y) = \int_{-x}^{+x}\int_{-y}^{+y} f(x,y)\, e^{-j2\pi(k_x x + k_y y)}\, dx\,dy$$

$$\text{since } f(x,y) \text{ is even both in x and y} : F(k_x,k_y) = 4\int_{0}^{x}\int_{0}^{y} f(x,y)\cos(2\pi k_x x)\cos(2\pi k_y y)\,dx\,dy$$

$$\text{for sampled data} : F(k_x,k_y) = 4\sum_{n=0}^{x/\Delta x}\sum_{m=0}^{y/\Delta y} f(n\Delta x, m\Delta y)\cos(2\pi k_x n\Delta x)\cos(2\pi k_y m\Delta y)$$

$$f(n\Delta x, m\Delta y) = \text{filter Weighting function} : W(n,m)$$

$$\text{for } \Delta x = \Delta y = 1 \text{ grid-unit} : F(k_x,k_y) = 4\sum_{n=0}^{x}\sum_{m=0}^{y} W(n,m)\cos(2\pi n k_x)\cos(2\pi m k_y)$$

FIG. 19.—Two-dimensional potential field filters.

An interesting sidelight of the Fourier transforms is the fact that the inverse transform will allow one to calculate the weighting function for any desired frequency content of the Second Vertical Derivative map. By specifying the frequency content desired, the inverse transform will therefore permit filter-design.

$$\text{POTENTIAL FIELD GIVEN BY} : \varphi(x,y,z)_{z=0} = \int_{-\infty}^{+\infty}\int_{-\infty}^{+\infty} \Phi(k_x,k_y)\, e^{j2\pi(k_x x + k_y y)}\, dk_x\,dk_y$$

$$\text{LAPLACE'S EQUATION} : \left(\frac{\partial^2\varphi}{\partial z^2}\right)_{z=0} = -\left(\frac{\partial^2\varphi}{\partial x^2} + \frac{\partial^2\varphi}{\partial y^2}\right)_{z=0}$$

$$\frac{\partial^2\varphi(x,y,z)}{\partial x^2} = -\int_{-\infty}^{+\infty}\int_{-\infty}^{+\infty} 4\pi^2 k_x^2\, \Phi(k_x,k_y)\, e^{j2\pi(k_x x + k_y y)}\, dk_x\,dk_y$$

$$\frac{\partial^2\varphi(x,y,z)}{\partial y^2} = -\int_{-\infty}^{+\infty}\int_{-\infty}^{+\infty} 4\pi^2 k_y^2\, \Phi(k_x,k_y)\, e^{j2\pi(k_x x + k_y y)}\, dk_x\,dk_y$$

$$\text{therefore} : \frac{\partial^2\varphi(x,y,z)}{\partial z^2} = \int_{-\infty}^{+\infty}\int_{-\infty}^{+\infty} 4\pi^2(k_x^2 + k_y^2)\, \Phi(k_x,k_y)\, e^{j2\pi(k_x x + k_y y)}\, dk_x\,dk_y$$

$$\text{or} : \text{TRANSFORM OF SECOND DERIVATIVE} : \Phi''(k_x,k_y) = 4\pi^2(k_x^2 + k_y^2)\,\Phi(k_x,k_y)$$

FUNDAMENTAL THEOREM:

$$\text{TRANSFORM OF DERIVATIVE OPERATOR} : F(k_x,k_y) = 4\pi^2(k_x^2 + k_y^2)$$

FIG. 20.—Fourier transform of ideal second vertical derivative.

We have seen how one can calculate the spatial frequency response of any of the numerical filter operators. Let us now turn to the response of the ideal Second Derivative Operator (Figure 20). Let a Potential Field be given by its two-dimensional Fourier transform. Laplace's equation states that the Second Derivative can be obtained by calculating the second horizontal derivatives in both x and y directions. The horizontal derivatives are calculated by differentiating the Fourier transform twice with respect to x and y and the expression for the Second Vertical Derivative results as shown in Figure 20. It will be noticed that the transform of the Second derivative is the same as that for the original field with the exception of the term $4\pi^2 (k_x^2 + k_y^2)$. Through the fundamental theorem for Fourier Transforms we know that the transform of the output equals the product of the transforms of input and filter, therefore the transform of the filter (Second Derivative) operator is equal to the term $4\pi^2 (k_x^2 + k_y^2)$.

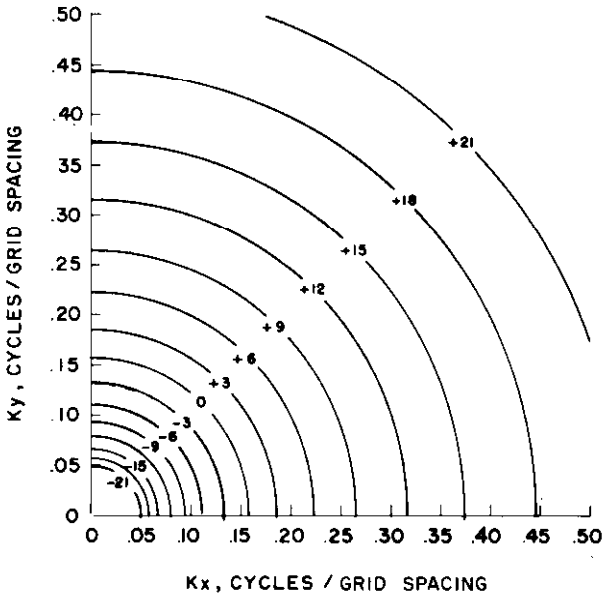


FIG. 21.—Amplitude response of "ideal" second vertical derivative filter (contours in db).

Figure 21 shows the Response of the ideal operator, as a function of the spatial frequency (wave-number) in both x and y directions, which may be described as a somewhat imperfect high-pass filter. Figure 22 is the response plot of an actual Second Derivative operator as calculated in the manner outlined previously. It will immediately be obvious that this is a very poor Second Derivative operator, particularly for the higher wave-number range. The large area of flat response would characterize this operator more closely as a band-pass filter.

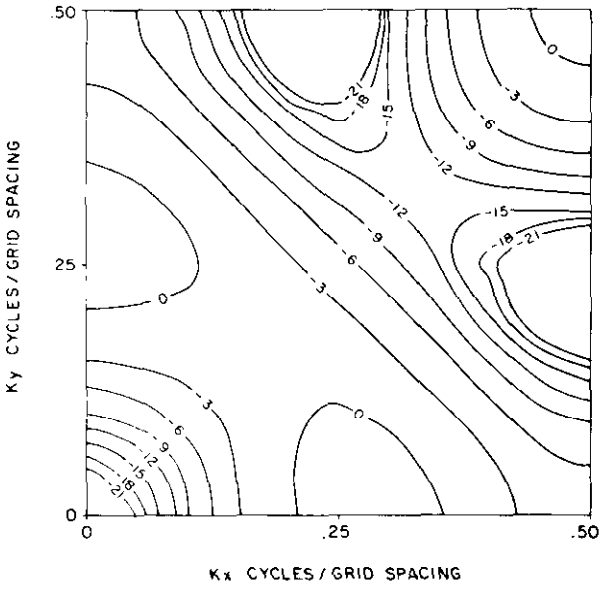


FIG. 22.—Amplitude response of a poor second vertical derivative operator (contours in db).

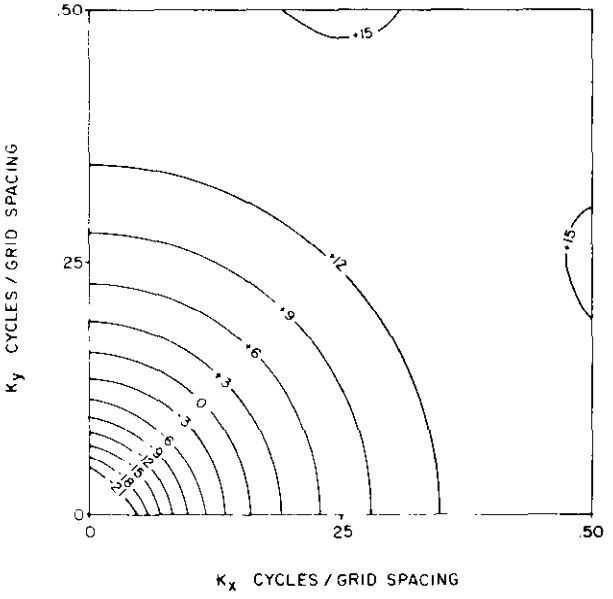


FIG. 23.—Amplitude response of a good second vertical derivative operator (contours in db).

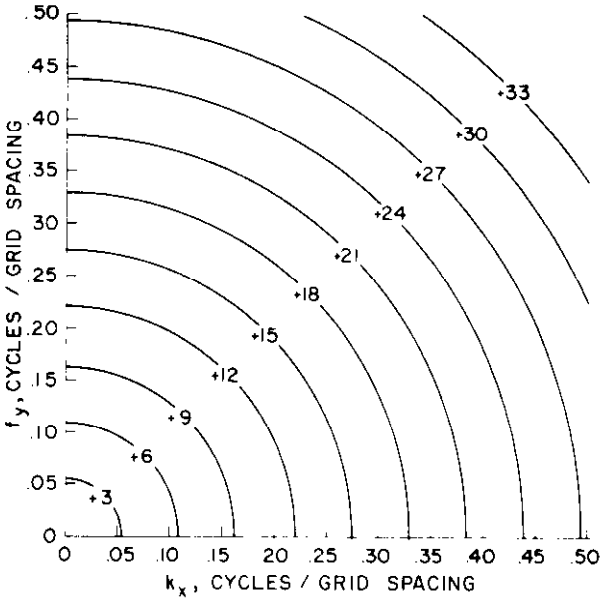


FIG. 24.—Amplitude response of "ideal" downward-continuation filter (contours in db).

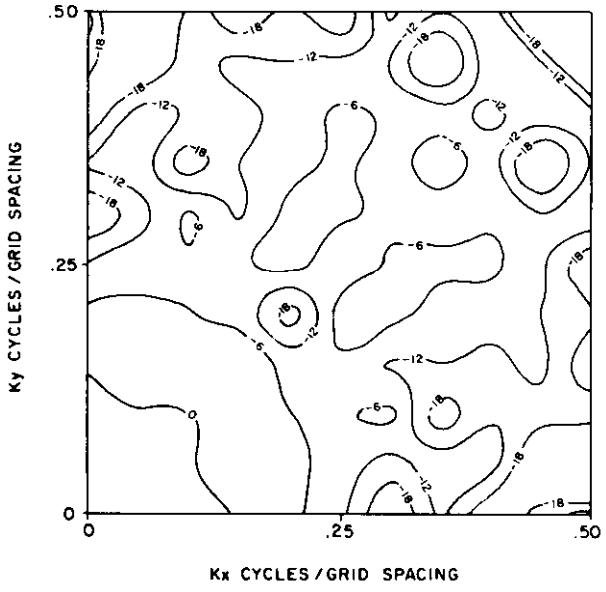


FIG. 25.—Amplitude response of poor downward continuation operator (contours in db).

Figure 23, on the other hand is an example of an excellent operator with a response much closer to the desired ideal one. Exactly the same reasoning as we followed for the Second Derivative, may be applied to the Downward Continuation operators. The actual response of the operator may be calculated through the Fourier transform of the particular weighting function and the "ideal" response may be obtained through transformation of the analytical expression for downward continuation. The desired response is shown in Figure 24 as calculated from the transform of the "ideal" (analytical) operator. Figure 25 illustrates the response of an actual downward continuation operator. It will be clear that this response only remotely resembles the desired result. Figure 26 however, is an example of a good operator, particularly in the lower wave-number range.

In summary therefore, we have seen how the two-dimensional Fourier transform is a necessity for the analysis of multi-channel filtering operations. Through the field of Industrial Optics, Fourier transformation has made possible the realization of the Laser Scan, essentially an optical multi-channel filter. Finally, the two-dimensional transform has been instrumental in quantifying Potential Field filtering operations, a result sorely needed for several decades. There exists little doubt that the future will see many more important exploration applications of the two-dimensional Fourier Transform.

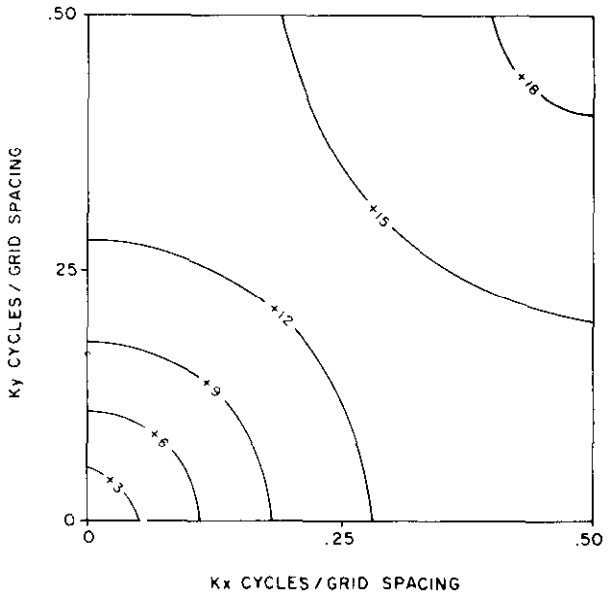


FIG. 26.—Amplitude response of good downward continuation operator

*APPENDIX*

A function f(t) may be expanded in a Fourier Series if it is periodic, piece-wise continuous and satisfies the relation:

$$\int_{-T/2}^{T/2} |f(t)|\, dt < \infty$$

The Fourier Series (complex case) then takes the following form:

$$f(t) \sum_{n=-\infty}^{+\infty} (A_n \cos\omega_n t + b_n \sin\omega_n t) \quad \ldots\ldots\ldots (1)\ *$$

where: $\omega_n = \frac{2\pi n}{T}$ , $n = \ldots -2, -1, 0, 1, 2 \ldots\ldots$

and T is the fundamental period

The coefficients $A_n$ and $B_n$ may be evaluated as follows:

$$A_n = \frac{1}{T} \int_{-T/2}^{T/2} f(t) \cos\omega_n t\, dt \quad \ldots\ldots\ldots\ldots\ldots (2a)$$

$$B_n = \frac{1}{T} \int_{-T/2}^{T/2} f(t) \sin\omega_n t\, dt \quad \ldots\ldots\ldots\ldots\ldots (2b)$$

According to well-known relationships:

$$\cos\omega_n t = \frac{1}{2} (e^{j\omega_n t} + e^{-j\omega_n t}) \quad \ldots\ldots\ldots\ldots\ldots (3a)$$

$$\sin\omega_n t = \frac{j}{2} (e^{j\omega_n t} - e^{-j\omega_n t}) \quad \ldots\ldots\ldots\ldots\ldots (3b)$$

where: $j = \sqrt{-1}$

Using these relationships (1) transforms to:

$$f(t) = \frac{1}{2} \sum_{n=-\infty}^{+\infty} [A_n (e^{j\omega_n t} + e^{-j\omega_n t}) + jB_n (e^{j\omega_n t} - e^{-j\omega_n t})] =$$

$$= \frac{1}{2} \sum_{n=-\infty}^{+\infty} [A_n - jB_n) e^{j\omega_n t} + (A_n + jB_n) e^{-j\omega_n t} \} \ldots\ldots\ldots (4)$$

*In the more general, complex case both positive and negative frequencies are considered.

We may further simplify (4) by realizing that for negative frequencies $\omega_n$:

$$A_{-n} = \frac{1}{T}\int_{-T/2}^{T/2} f(t)\cos(-\omega_n t)\,dt = A_n \quad \text{(even function)}$$

$$B_{-n} = \frac{1}{T}\int_{-T/2}^{T/2} f(t)\sin(-\omega_n t)\,dt = -B_n \quad \text{(odd function)}$$

Therefore (4) simplifies to:

$$f(t) = \sum_{n=-\infty}^{\infty} F_n e^{j\omega_n t} \qquad \ldots\ldots(5)$$

where: $F_n = \frac{1}{2}(A_n - jB_n)$ $\ldots\ldots(6)$

Combining these various forms we obtain (substituting (2a) and (2b) in (6) )

$$F_n = \frac{1}{T}\int_{-T/2}^{T/2} f(t)\, e^{-j\omega_n t}dt,$$

the desired result.

*BIBLIOGRAPHY*

DOBRIN, M. B., INGALLS, A. L. and LONG, J. A., *"Velocity and Frequency Filtering of Seismic Data using Laser Light,"* Geophysics, Vol. 30, Dec. 1965, pp. 1144-1178.

DARBY, E. K., DAVIES, E. B., *"Analysis and Design of Two-dimensional Filters for Two-dimensional Data,"* Geophysical Prospecting, Vol. 15, Sept. 1967, pp. 383-406.

ZURFLUEH, E. G., *"Applications of Two-dimensional Linear Wave-length Filtering,"* Geophysics, Vol. 32, No. 6, Dec. 1967, pp. 1015-1035.

FULLER, B. D., *"Two-dimensional Frequency Analysis of Grid Operators,"* Preprint 36th Meeting of the SEG, University of California, Berkeley.